

# Micro-Raman Mapping of 3C-SiC Thin Films Grown by Solid–Gas Phase Epitaxy on Si (111)

T. S. Perova · J. Wasyluk · S. A. Kukushkin ·  
A. V. Osipov · N. A. Feoktistov · S. A. Grudinkin

Received: 5 May 2010 / Accepted: 7 June 2010 / Published online: 20 June 2010  
© The Author(s) 2010. This article is published with open access at Springerlink.com

**Abstract** A series of 3C-SiC films have been grown by a novel method of solid–gas phase epitaxy and studied by Raman scattering and scanning electron microscopy (SEM). It is shown that during the epitaxial growth in an atmosphere of CO, 3C-SiC films of high crystalline quality, with a thickness of 20 nm up to few hundreds nanometers can be formed on a (111) Si wafer, with a simultaneous growth of voids in the silicon substrate under the SiC film. The presence of these voids has been confirmed by SEM and micro-Raman line-mapping experiments. A significant enhancement of the Raman signal was observed in SiC films grown above the voids, and the mechanisms responsible for this enhancement are discussed.

**Keywords** 3C-SiC · Voids in SiC ·  
Micro-Raman spectroscopy · Micro-Raman mapping

## Introduction

Silicon carbide (SiC) is a very attractive material for the fabrication of microelectronic and optoelectronic devices due to its wide bandgap, high thermal conductivity,

excellent thermal and chemical stability and its resistance to radiation damage and electrical breakdown [1]. SiC has over 170 different polytypes [2]. The most common forms are 4H, 6H, known as the hexagonal ( $\alpha$ -SiC) types, and the cubic 3C-SiC type [2–5]. Among the various polytypes, the 3C-SiC variety possesses unique properties, including a high electron mobility up to  $1000 \text{ cm}^2/\text{Vs}$  and a consequent high saturation drift velocity. 3C-SiC can be used as a buffer layer for the subsequent heteroepitaxial growth of gallium nitride and other group III-nitrides [6]. Because of the small lattice mismatch between SiC and gallium nitride (GaN), 6H-SiC can also act as a substrate for the epitaxial growth of GaN [7], which has application in blue and violet light-emitting diodes and lasers. Therefore, reproducible growth of SiC on silicon wafers is a very important issue for the semiconductor and MEMS industry.

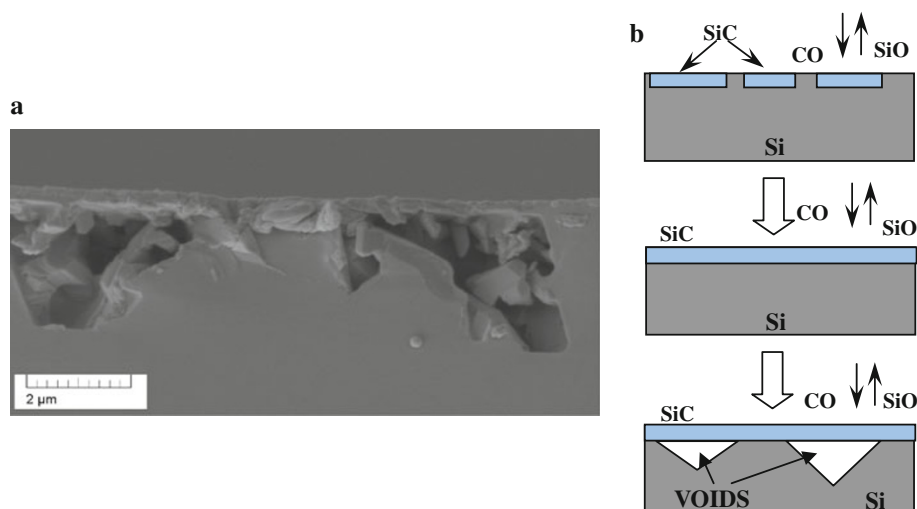
The theoretical and experimental basis for a new method of solid–gas phase epitaxy of different polytypes of SiC on Si has been demonstrated recently in Refs. [8, 9]. The essence of the approach is that during SiC seed formation, simultaneous growth of pores, or voids, from the vacancies occurs (see Fig. 1b). These voids provide an optimum relaxation of elastic strain and, in this case, misfit dislocations are not formed, in contrast to traditional techniques using a mixture of gases. The voids typically have an inverted pyramid or rectangular shape when using (111) Si or (100) Si, respectively. Formation of voids, visible using SEM and TEM methods, at the initial stage of SiC film growth on Si substrates has already been discussed in the literature [10–13]. The formation of voids discussed in the present investigation is different, since the voids formed are not hollow (see Fig. 1a), but filled with a type of SiC material attached to the Si (110) and (-211) planes inside the voids. Micro-Raman mapping experiments were used in this study for the first time, in order to investigate the

T. S. Perova (✉) · J. Wasyluk  
Department of Electronic and Electrical Engineering, University  
of Dublin, Trinity College, Dublin 2, Ireland  
e-mail: perovat@tcd.ie

S. A. Kukushkin · A. V. Osipov  
Institute of Problems of Mechanical Engineering, Russian  
Academy of Sciences IPME RAS, Bolshoy 61, V.O.,  
199178 St. Petersburg, Russia

N. A. Feoktistov · S. A. Grudinkin  
Ioffe Physical Technical Institute, Polytechnicheskaya ul.,  
26, 194021 St. Petersburg, Russia

**Fig. 1** **a** SEM image of sample SiC/(111)Si and **b** schematic model of void formation during SiC growth



structural properties of the SiC film grown on the Si substrate and also on top of the voids.

## Experimental

A low-pressure CVD system with a vertical cold-wall reactor made from sapphire, with a diameter of 40 mm and length of 50 mm, in which the central zone was heated, was used for SiC film deposition. The silicon wafer was placed on a graphite holder, with a thermocouple attached to the end. The sapphire tube was connected to a high vacuum system, consisting of diffusion and turbo-molecular pumps. Initially, the system was pumped down to a pressure of  $10^{-5}$ – $10^{-6}$  Torr. For SiC deposition, a 2' (111)-orientated Si substrate with a thickness of 300  $\mu\text{m}$  and a tilt of  $4^\circ$  was used. Growth of SiC films on Si(111) was achieved using the chemical reaction of monocrystalline silicon and CO gas, supplied at a rate of 1–10  $\text{ncm}^3/\text{min}$  and a pressure of 0.1–10 Torr. Growth occurs in the temperature range 1100–1350°C, and growth durations of 10–60 min were used. Due to the fabrication procedure, the SiC samples obtained are mainly lightly doped with nitrogen at a level of  $10^{14} \text{ cm}^{-3}$ .

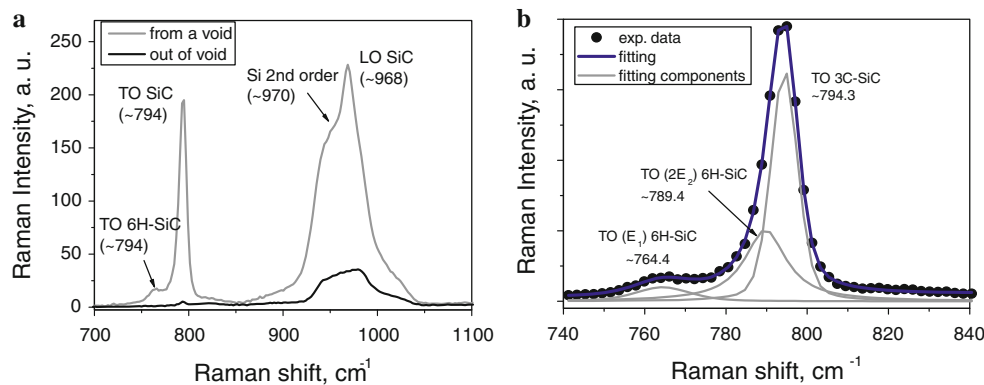
Raman spectroscopy is a powerful technique for the characterisation of SiC structures in particular, since it allows the identification of various polytypes [2–5]. The Raman efficiency of SiC is sufficiently high because of the strong covalent bonds in the material. In addition, Raman spectral parameters such as peak position, intensity, line-width and polarisation provide useful information on the crystal quality [14]. Raman spectra were registered in a backscattering geometry using a RENISHAW 1000 micro-Raman system equipped with a CCD camera and a Leica microscope. Two types of measurements were performed: single-spot measurements from both a void area and

outside the void area in the SiC layers, and line-mapping measurements conducted along the voids with nanoscale depth profile of the void varied from 30 nm up to 2000 nm (at the centre of void). For single measurements, an  $\text{Ar}^+$  laser at 457 nm with a power of 10 mW was used as the excitation source, while for line mapping an excitation wavelength of 633 nm from a HeNe laser with a laser power of 10 mW was used. Line mapping was performed at a distance,  $x$ , ranging from 0 to 13  $\mu\text{m}$  with an in-plane step size of 300 nm, where zero corresponds to the starting point of the measurements. Laser radiation was focused onto the sample using a 100 $\times$  microscope objective with a short-focus working distance, providing a spot size of  $\sim 600$  nm. Cross-sectional morphologies of the SiC films were characterised with a Tescan Mira SEM.

## Results and Discussions

Figure 2 shows a representative Raman spectra from a SiC film on Si (111) measured at the void and outside the void. The feature seen in the range 900–1100  $\text{cm}^{-1}$  is associated with second-order Raman scattering from the Si [15]. The characteristic transverse optical (TO) and longitudinal optical (LO) phonon modes are observed at  $\sim 794 \text{ cm}^{-1}$  and  $\sim 968 \text{ cm}^{-1}$ , respectively. This confirms that the SiC layers analysed in this work mainly consist of a cubic polytype structure [5, 16]. A low intensity shoulder, clearly observed at  $\sim 764 \text{ cm}^{-1}$  near the TO band, indicates the presence of a small amount of the 6H-SiC polytype in this SiC layer. From Fig. 2a and b, the TO peak at  $794 \text{ cm}^{-1}$  demonstrates asymmetry from the low-frequency side. At the same time, in accordance with Nakashima [5], structural disorder in the SiC leads to a symmetrical widening of all the TO peaks. We conclude that the observed asymmetry of the TO peak is due to the presence of a 6H-SiC

**Fig. 2** **a** Raman spectra from SiC layer grown on Si substrate measured at the void area and outside the void area. **b** Fitting of TO band from Raman spectrum, detected at the void, with three functions (Lorentzian + Gaussian)



peak at  $\sim 789 \text{ cm}^{-1}$ , clearly demonstrated by fitting of the TO band in Fig. 2b. From the fit, the linewidth of the band at  $\sim 794 \text{ cm}^{-1}$  is approximately  $\sim 7.8 \text{ cm}^{-1}$ . This is  $2.5 \text{ cm}^{-1}$  larger than that for relaxed 3C-SiC on a 6H-SiC substrate in Ref. [17]. This relatively small difference in linewidth leads to the conclusion that the thin SiC layer grown on Si (111) has reasonably good crystalline quality; this was confirmed by energy dispersive X-ray analysis in Ref. [17].

A large enhancement of the Raman peak intensity, by up to 40 times for some samples, for both TO and LO modes, is observed at the void area. This enhancement enables the acquisition of a reasonably good Raman spectrum from ultra-thin SiC layers, as shown in Fig. 2a. Three mechanisms can contribute to the observed enhancement of Raman signal: (a) multiple reflection of the incident light inside the void, (b) multiple reflection of the Raman signal in the SiC layer on top of the void and (c) the presence of additional SiC material grown on the (110) Si ribs of the pyramid inside the voids [9, 10, 18]. The first mechanism is also responsible for the moderate enhancement of the Si second-order peak, by approximately 4 times, from the Si ribs. A somewhat similar effect was discussed for porous Si and SiC in Refs. [19, 20]. For the second mechanism, the enhancement of the Raman signal in thin films, surrounded by media with low refractive indices, was discussed recently in Ref. [21] for graphene. We use a similar approach for the estimation of the effect of multiple reflections of the Raman signal on the peak intensity from the thin film using a three-layer model consisting of SiC–air–silicon. This model will be discussed together with the line-mapping results in the next paragraph.

Figure 3a presents an optical microscopy image of a 3C-SiC/Si sample, where the brighter dots correspond to the voids seen under thin SiC layers. The arrow on Fig. 3a shows the route of the line-mapping measurements. The Raman mapping was performed at the different depth of the void varied from 30 nm up to 2000 nm (correspondent to the centre of the void). Figure 3b, c and d show Raman line-maps for the peak position, peak intensity and

linewidth of the SiC-TO peak along the voids for the 3C-SiC/Si sample. Note that not all the points, collected during mapping experiment, are shown in these figures for the clarity of presentation. Since the TO peak position is more sensitive to the stress relaxation effect [19], the TO-SiC peak was used to study the relaxation level in 3C-SiC films with different thicknesses and void size. The peak position of the SiC-TO band in a relaxed 3C-SiC structure is typically located at  $796 \text{ cm}^{-1}$ , but for SiC layers grown on Si, the TO band shifts to the low-frequency side [16]. We observed the TO-SiC peak position at around  $794 \text{ cm}^{-1}$ , indicating that the SiC layer is under stress. Tensile stress in the SiC layer is observed since the lattice constant for SiC ( $a_{\text{SiC}} = 4.3 \text{ \AA}$ ) is less than that for Si ( $a_{\text{Si}} = 5.38 \text{ \AA}$ ). Figure 3b presents the peak position of the TO-SiC peak as a function of distance,  $x$ . From this figure, the peak position varies from  $794.5 \text{ cm}^{-1}$  at the middle of the void to  $793.5 \text{ cm}^{-1}$  outside the voids. A larger tensile stress is observed outside the voids than at voids, confirming that stress relief is occurring at the cavities. Figure 3d shows the full width at half maximum (FWHM) of the SiC-TO mode as a function of mapping distance. The linewidth of the TO peak significantly increases at the cavities (by  $\sim 3 \text{ cm}^{-1}$ ), a result of the contribution of differently oriented SiC materials inside the void as mentioned earlier.

The strong enhancement of the Raman peak intensity of the SiC-TO mode, by a factor of 20, inside the cavities is confirmed by the line-mapping measurements presented in Fig. 3c. It can be seen that the enhancement is significantly larger at the centre of the voids, corresponding to a larger cavity depth or a thicker air layer (see Fig. 1). By considering the multiple reflection of the Raman signal based on Fresnel's equation [21], and by varying the thickness of the air layer from 0 to 2000 nm and the thickness of the SiC layer between 0 and 800 nm, we estimated the Raman enhancement at the centre of the void to be approximately 10 times larger than that at the edge of the void for a SiC layer with a thickness of about 120 nm (details of these calculations will be published elsewhere [22]). An increase

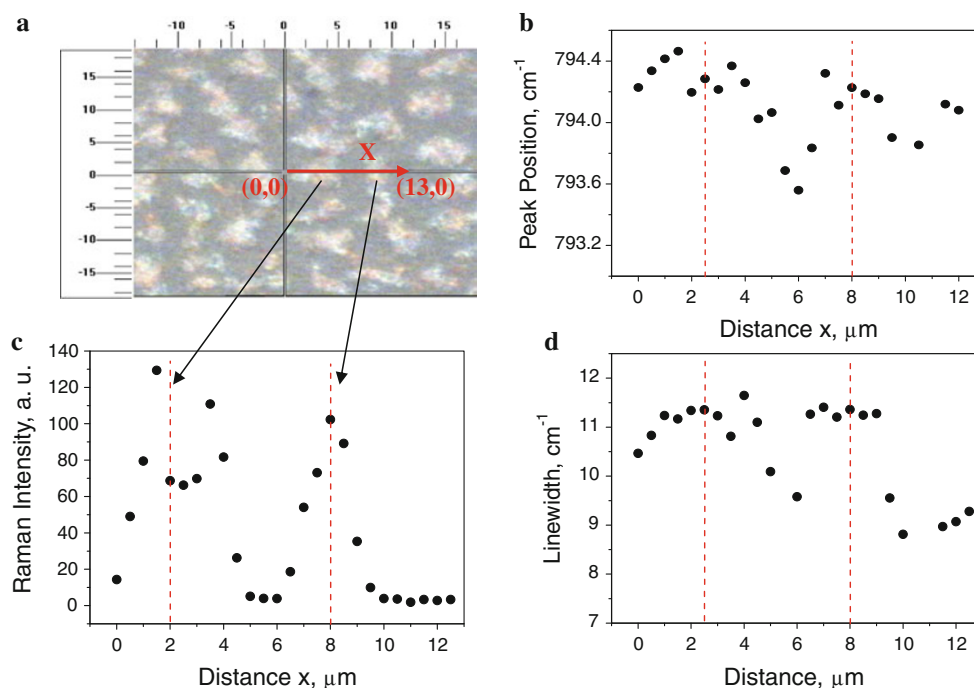


**Fig. 3** **a** Top view of the sample of 3C-SiC obtained by optical microscopy (scale in  $\mu\text{m}$ ), the red arrow shows the mapping line. Results of Raman line mapping for **b** peak position, **c** linewidth and

**d** peak intensity of the TO phonon mode for the 3C-SiC/Si sample (dashed lines correspond to the centres of the voids)

in the layer thickness to 800 nm reduces the Raman signal enhancement by a factor of  $\sim 5$ . This was confirmed experimentally by Raman line-mapping measurements for the sample with an  $\sim 800\text{-nm}$ -thick SiC layer, where enhancement of the Raman signal by a factor of only two was detected at the void centre.

## Conclusion

In summary, the presence of voids during the growth of thin SiC layers by solid-gas phase epitaxy has been confirmed experimentally by scanning electron microscopy and micro-Raman spectroscopy. The Raman line-mapping experiments presented in this work confirm that the voids formed in the Si substrate under the SiC layer cause relaxation of the elastic stress caused by lattice mismatch between the SiC and Si. It is shown that the SiC layers investigated here are composed mainly of the cubic polytype of SiC, with small amounts of 6H-SiC. It is worth mentioning that in accordance with Ref. [23], the quality of GaN layers grown on SiC layers consisting of a mixture of the cubic and hexagonal polytype is better than that for GaN layers grown on a single SiC polytype. A strong enhancement in the peak intensity of the TO and LO modes is observed for the Raman signal measured at the voids.

**Acknowledgments** J. Wasyluk would like to acknowledge the financial support of the IRCSET Ireland (Postgraduate Award) and ICGEE Programme. The study has been performed with financial support from the Russian Foundation for Fundamental Research (grants 07-08-00542, 09-03-00596 and 08-08-12116-ofi) and the RAS Program: «Basis of Fundamental Research in Nanotechnologies and Nanomaterials». S. Dyakov is acknowledged for performing the calculation of Raman enhancement.

**Open Access** This article is distributed under the terms of the Creative Commons Attribution Noncommercial License which permits any noncommercial use, distribution, and reproduction in any medium, provided the original author(s) and source are credited.

## References

- O. Kordina, L.O. Björketun, A. Herry, C. Hallin, R.C. Glass, L. Hultman, J.E. Sundgren, E. Janzen, *J. Cryst. Growth* **154**, 303 (1995)
- M.J. Pelletier, *Analytical applications of Raman spectroscopy* (Blackwell Science, UK, 1999)
- S. Nakashima, K. Tahara, *Phys. Rev. B* **40**, 6339 (1989)
- S. Nakashima, H. Harima, T. Tomita, T. Suemoto, *Phys. Rev. B* **62**, 16605 (2000)
- S. Nakashima, H. Harima, *Phys. Stat. Sol. A* **162**, 39 (1997)
- T. Takeuchi, H. Amano, K. Hiramatsu, N. Sawaki, I. Akasaki, *J. Cryst. Growth* **115**, 634 (1991)
- A.S. Zubrilov, Yu.V. Melnik, A.E. Nikolaev, *Semiconductors* **33**, 1067 (1999)
- S.A. Kukushkin, A.V. Osipov, N.A. Feoktistov, Patent RF No 2008102398, filed on 22 January (2008)
- S.A. Kukushkin, A.V. Osipov, *Phys. Solid State* **50**, 1238 (2008)

10. R. Scholz, U. Gösele, E. Niemann, F. Wischmeyer, *Appl. Phys. A* **64**, 115 (1997)
11. A. Severino, G. D'Arrigo, C. Bongiorno, S. Scalese, F. La Via, G. Foti, *J. Appl. Phys.* **102**, 023518 (2007)
12. J.P. Li, A.J. Steckl, *J. Electrochem. Soc.* **142**, 2 (1995)
13. W. Attenberger, J. Lindner, V. Cimalla, J. Pezoldt, *Mater. Sci. Eng. B* **61/62**, 544 (1999)
14. W.J. Choyke, H. Matsunami, G. Pensl, V.I. Taylor, Francis, *Silicon Carbide—A review of fundamental questions and applications to current device technology*, (1997)
15. P.A. Temple, C.E. Hathaway, *Phys. Rev. B* **7**, 3685 (1973)
16. Z.C. Feng, W.J. Choyke, J.A. Powell, *J. Appl. Phys.* **64**, 6827 (1988)
17. J. Wasyluk, T.S. Perova, S.A. Kukushkin, A.V. Osipov, N.A. Feoktistov, S.A. Grudinkin, *Mater. Sci. Forum* **645–648**, 359 (2010)
18. L.M. Sorokin, N.V. Veselov, M.P. Shcheglov, A.E. Kalmykov, A.A. Sitnikova, N.A. Feoktistov, A.V. Osipov, S.A. Kukushkin, *Techn. Phys. Lett.* **34**, 992 (2008)
19. V. Lysenko, D. Barbier, B. Champagnon, *Appl. Phys. Lett.* **79**, 2366 (2001)
20. I. Gregora, B. Champagnon, L. Saviot, Y. Monin, *Thin Solid Film* **255**, 139 (1995)
21. Y.Y. Wang, Z.H. Ni, Z.X. Shen, H.M. Wang, Y.H. Wu, *Appl. Phys. Lett.* **92**, 043121 (2008)
22. S. Dyakov, J. Wasyluk, T.S. Perova, (in preparation)
23. I.G. Aksyanov, V.N. Bessolov, Yu.V. Zhilyaev, M.E. Kompan, E.V. Konenkova, S.A. Kukushkin, A.V. Osipov, N.A. Feoktistov, Sh. Sharofidinov, M.P. Shcheglov, *Semiconductors* (submitted for publication)